The Technology and Applications of Selective Oxidation of AlGaAs

Kent D. Choquette, K. M. Geib, and H. Q. Hou
Center for Compound Semiconductor Science and Technology
Sandia National Laboratories
Albuquerque, NM 87185-0603

D. Mathes and Robert Hull
University of Virginia
Charlottesville, VA

Wet oxidation of AlGaAs alloys, pioneered at the University of Illinois a decade ago, recently has been used to fabricate high performance vertical-cavity surface emitting lasers (VCSELs). The superior properties of oxide-confined VCSELs has stimulated interest in understanding the fundamentals of wet oxidation. We briefly review the technology of selective oxidation of III-V alloys, including the oxide microstructure and oxidation processing as well as describe its application to selectively oxidized VCSELs.

A. Introduction

Wet oxidation of AlAs was first reported in 1979, although the native (Gibbsite) oxide phase was formed at the low oxidation temperature used (100°C) [1]. Ten years later during studies of atmospheric degradation of AlAs, it was discovered by researchers at the University of Illinois that wet oxidation of Al-containing semiconductors (AlGaAs, AlInAs, AlGaInP, etc.) at temperatures above ≈300 °C produces a mechanically robust oxide with a low refractive index [2]. The utility of this oxide was initially demonstrated in a variety of edge emitting laser structures where the oxide layers provide both index-guiding and buried current apertures [3-5].

Oxidized AlGaAs layers have also recently been introduced within vertical cavity surface emitting lasers (VCSELs) [6,7]. Selectively oxidized VCSELs have exhibited superior laser performance due to the efficient electrical and optical confinement afforded by the buried oxide layers. Other applications of wet oxidized AlGaAs have included high index contrast distributed Bragg reflector mirrors [8], birefringent optical waveguides [9], buried microlenses [10], and metal-insulator-semiconductor transistors [11]. Nevertheless as shown in Fig. 1, research on the oxidation of III-V alloys as measured by journal publications has been driven over the past few years by the significant interest in selectively oxidized VCSELs. Understanding the microstructure and processing of oxides converted from AlGaAs is essential for the development of a robust fabrication technology for optoelectronic devices [12]. We briefly review selective wet oxidation of AlGaAs alloys and its application to VCSEL fabrication.
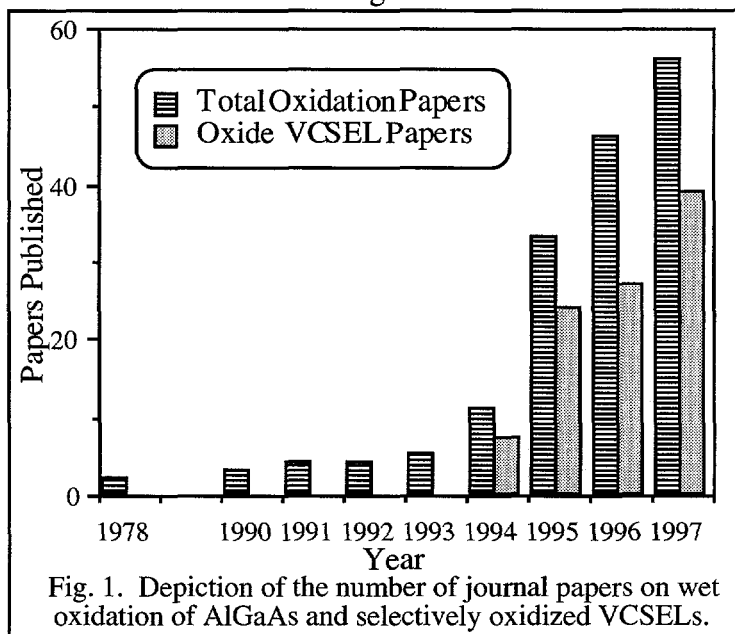

Fig. 1. Depiction of the number of journal papers on wet oxidation of AlGaAs and selectively oxidized VCSELs.

DISCLAIMER

DISCLAIMER

Portions of this document may be illegible electronic image products. Images are produced from the best available original document.

B. Oxide Microstructure

Cross section transmission electron microscopy (TEM) has been applied to characterize the microstructure of buried oxide layers as shown in Fig. 2. Electron diffraction patterns indicate that the oxide converted from AlGaAs is an amorphous solid solution of $(Al_xGa_{1-x})_2O_3$ [13]. The bright field image in Fig. 2 reveals only granular amorphous contrast within the oxide, with an ≈ 17 nm thick interface zone at the oxide/semiconductor interface. No extended defects are

Fig. 2. Cross section TEM image of an amorphous oxide layer converted from 100 nm thick AlAs surrounded by GaAs layers.

apparent along the oxide/semiconductor interfaces and a smooth transition over several lattice constants is apparent between the oxide and semiconductor.

The thickness of an oxide formed at temperatures above 300 °C tends to be reduced compared to the original semiconductor layer [2]. The linear shrinkage is measured to be 12 to 13% in the amorphous oxide layers converted from AlAs [8]. However, shrinkage for oxidized $Al_{0.92}Ga_{0.08}As$ layers is measured to be only 6.7% [14]. The reduced thickness of the oxide is thus dependent upon composition of the converted semiconductor and can result in strain fields at the oxide terminus [15].

C. Oxidation Processing

To develop a manufacturable wet oxidation technique, the influence of process parameters such as gas flow, gas composition, temperature, Al composition, and layer thickness on the rate of oxidation have been examined [12,16]. The lateral oxidation has a linear oxidation rate which obeys an Arrhenius temperature dependence. A strong compositional dependence of the oxidation rates is shown in Fig. 3(a) where the oxidation rate of $Al_xGa_{1-x}As$ for x varying from 1 to 0.84, changes by more than 2 orders of magnitude [7]. It is this oxidation selectivity which can be exploited for the fabrication of buried oxide layers within a VCSEL; with minute changes of Ga concentration, specific or multiple AlGaAs layer(s) can be selected out to form buried oxide layers for electrical and optical confinement (see Fig. 5).

The thickness of the semiconductor layer to be oxidized can also influence its oxidation rate as shown in Fig. 3(b). For thickness ≥ 60 nm, a relatively constant lateral oxidation rate is observed; for thinner layers the oxidation rate dramatically decreases. Comparing Figs. 3(a) and 3(b), it is obvious that the oxidation rate dependence on thickness can compensate for the compositional dependence: thin layers of AlAs may oxidize slower than thick layers of AlGaAs.

Finally, the composition of the surrounding layers will affect the oxidation rate and shape of the oxide terminus through diffusion and supply of reactants [17]. For example as shown in Fig. 4, a rapidly oxidizing layer can supply reactants to its surrounding layers such that significant vertical oxidation into the adjoining layers occurs. Fig. 4 shows a tapered oxide terminus which results from the oxidation of a 14 nm thick $Al_{0.98}Ga_{0.02}As$ layer embedded within a thicker $Al_{0.92}Ga_{0.08}As$ layer. The effective lateral oxidation rate of the $Al_{0.92}Ga_{0.08}As$ layer in Fig. 12 is enhanced by a factor of 2 over the rate predicted from Fig. 3(a) due to vertical oxidation originating from exposure to reactants supplied from the thin oxidized $Al_{0.98}Ga_{0.02}As$ layer.
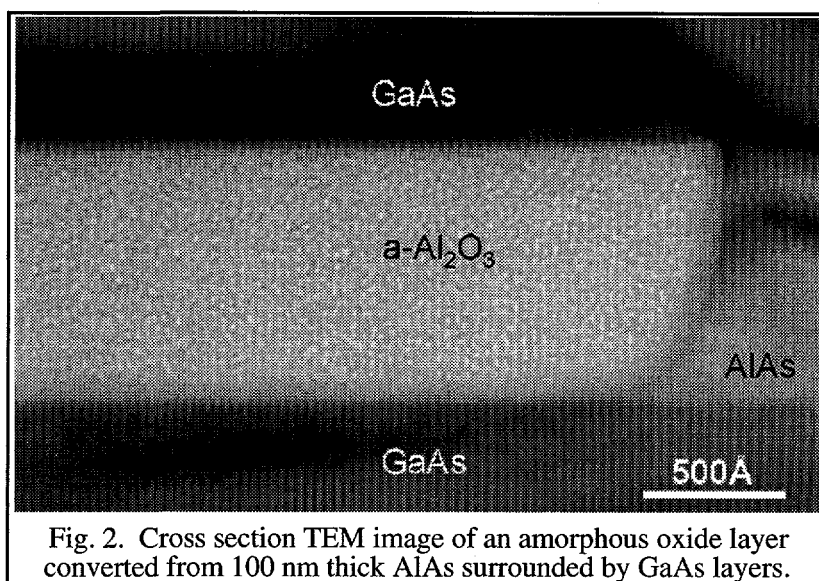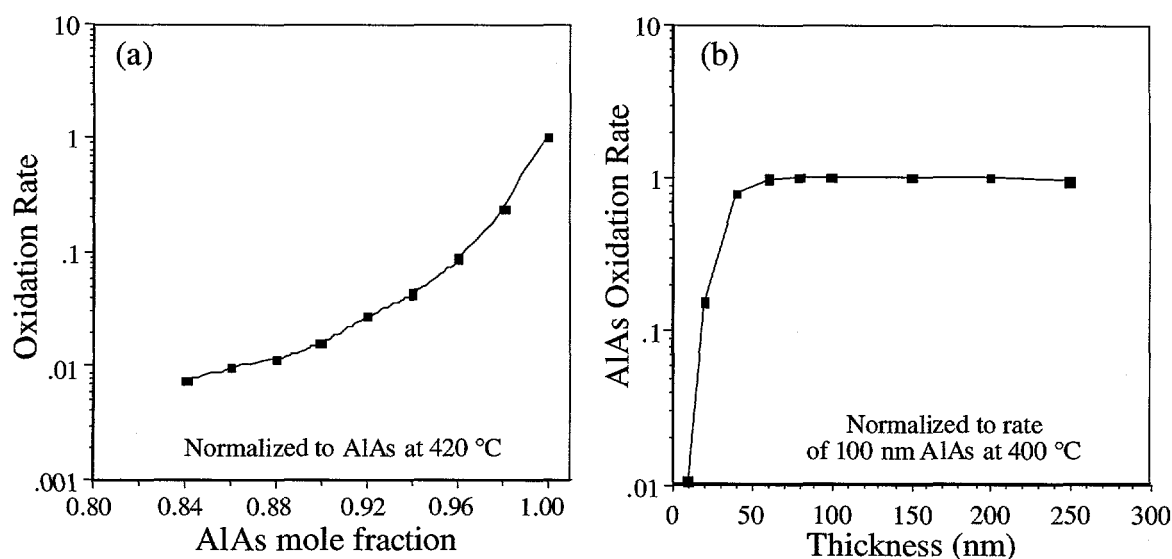
Fig. 3. (a) Normalized $Al_xGa_{1-x}As$ oxidation rate at 420 °C versus composition; (b) normalized oxidation rate of AlAs at 400 °C versus layer thickness.

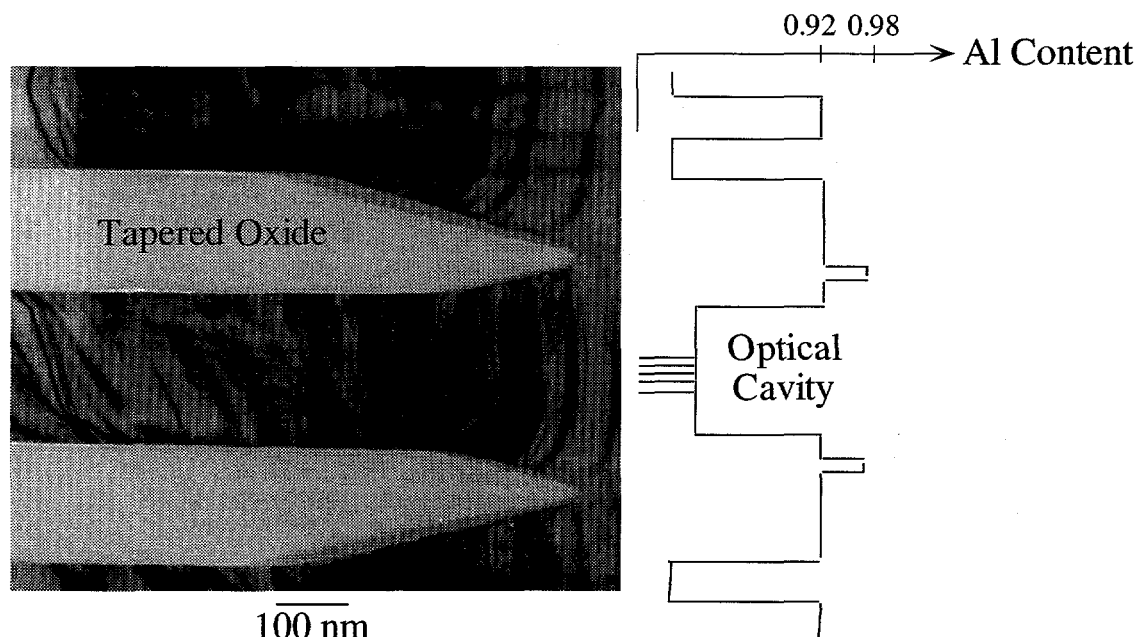Fig. 4. Cross section TEM image of two tapered oxides (adjacent to optical cavity) produced from 14 nm thick $Al_{0.98}Ga_{0.02}As$ embedded within a 160 nm thick $Al_{0.92}Ga_{0.08}As$ layer.

D. Selectively Oxidized VCSELs

Significant performance advances have been achieved from selectively oxidized VCSELs which, as depicted in Fig. 5, incorporate one or more buried oxide apertures for efficient electrical and optical confinement [7,18]. These devices are fabricated by first growing the material by metalorganic vapor phase epitaxy. A mesa is etched to expose the sidewalls for oxidation as sketched in Fig. 5. The lateral extent of oxidation within the laser mesa can be controlled by the oxidation time [18]. Moreover, through design of the composition of the various layers within the VCSEL, the oxidation profile within the laser cavity can be tailored to affect the optical confinement and/or electrical injection into the laser.
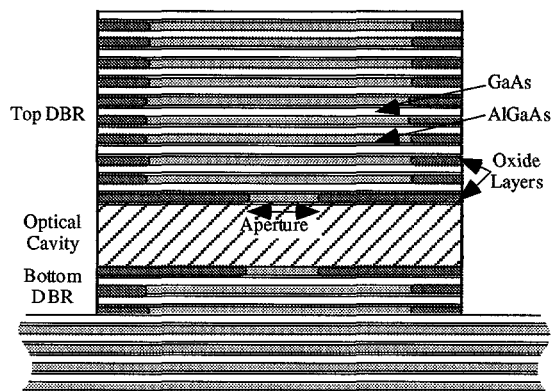
Fig. 5. Selectively oxidized VCSEL composed of GaAs/AlGaAs multilayers and buried oxide layers.
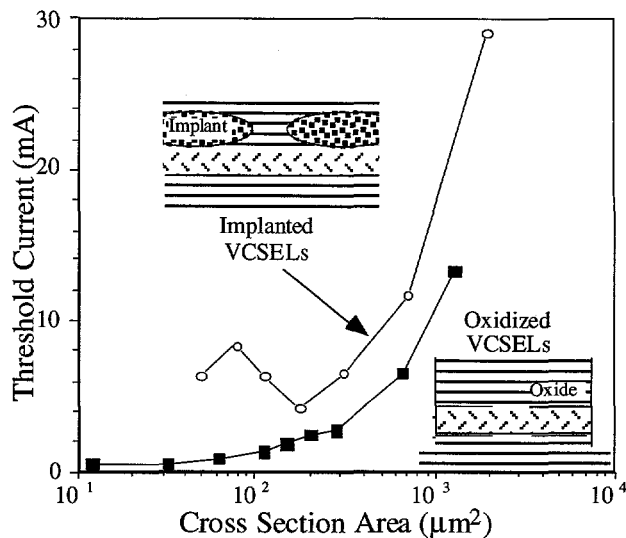

Fig. 6. Comparison of threshold current of implanted and selectively oxidized VCSELs.

The improved electrical confinement arising from the oxide apertures is particularly manifest as reduced threshold current and voltage compared to other VCSEL structures [19]. In Fig. 6 we compare selectively oxidized and ion implanted 850 nm VCSELs with various cavity sizes fabricated from the same epitaxial wafer. The ion implanted VCSELs rely on ion implantation to render a region around the laser nonconductive, thus defining the laser cavity. The reduced threshold current for the selectively oxidized VCSELs in Fig. 6 arises due to the improved electrical confinement and reduced current spreading. Moreover, the refractive index of the buried oxide layer changes from 3.0 for the original AlGaAs layer to ≈1.6 for the oxidized layer. This induces a significant index difference between the laser cavity and the region surrounding the laser thus providing index-guiding optical confinement. The ion implanted VCSELs in Fig. 6 do not exhibit monotonic decreasing threshold current with decreasing size, due to increased diffraction loss. In contrast, the index-guiding in the selectively oxidized VCSELs produces a monotonic decrease of the threshold currents in Fig. 6. Selectively oxidized VCSELs have also demonstrated high power conversion efficiency [20], high output power, and high speed modulation [21].

E.   Conclusion

Further work will certainly be required to develop selective wet oxidation of AlGaAs into a manufacturing technology for VCSELs or other microelectronic/photonic devices. Although selective oxidation has been shown to be a stable fabrication process, in order to scale up to full wafer manufacture, issues pertaining to reproducibility and uniformity obviously remain. Moreover, developing a means to photolithographically predefine the length of the oxide layer within a given device structure would be advantageous. Finally, analogous to process simulators available for Si oxidation, it will be necessary to develop predictive models of the oxidation of AlGaAs. In spite of these remaining challenges, the motivation to develop a wet oxidation technology is clearly driven by the demonstrated high performance of selectively oxidized VCSELs. Therefore, to meet the requirements of emerging applications, selective wet oxidation of AlGaAs may play an important role in the manufacture of high performance VCSELs.

References

[1] W. T. Tsang, *Appl. Phys. Lett.*, 1978, vol. 33, 426.

[2] J. M. Dallesasse, N. Holonyak, Jr., A. R. Sugg, T. A. Richard, and N. El-Zein, *Appl. Phys. Lett.*, 1990, vol. 57, 2844.

[3] J. M. Dallesasse and N. Holonyak, Jr., *Appl. Phys. Lett.*, 1991, vol. 58, 394.

[4] F. A. Kish, S. J. Caracci, N. Holonyak, Jr., J. M. Dallesasse, K. C. Hsieh, M. J. Ries, S. C. Smith, and R. D. Burnham, *Appl. Phys. Lett.*, 1991, vol. 59, 1755.

[5] S. A. Maranowski, A. R. Sugg, E. I. Chen, and N. Holonyak, Jr., *Appl. Phys. Lett.*, 1993, vol. 63, 1660.

[6] D. L. Huffaker, D. G. Deppe, K. Kumar, and T. J. Rogers, *Appl. Phys. Lett.*, 1994, vol. 65, 97.

[7] K. D. Choquette, R. P. Schneider, Jr., K. L. Lear, and K. M. Geib, *Electron. Lett.*, 1994, vol. 30, 2043.

[8] M. H. MacDougal, H. Zhao, P. D. Dapkus, M. Ziari, and W. H. Steier, *Electron. Lett.*, 1994, vol. 30, 1147.

[9] A. Flore, V. Berger, E. Rosencher, N. Laurent, S. Theilmann, N. Vodjdani, and J. Nagle, *Appl. Phys. Lett.*, 1996, vol. 68, 1320.

[10] O. Blum, K. L. Lear, H. Q. Hou, and M. E. Warren, *Electron. Lett.*, 1996, vol. 32, 1406.

[11] E. I. Chen, N. Holonyak, Jr., and S. A. Maranowski, *Appl. Phys. Lett.*, 1995, vol. 66, 2688.

[12] K. D. Choquette, K. M. Geib, C. I. H. Ashby, R. D. Twesten, O. Blum, H. Q. Hou, D. M. Follstaedt, B. E. Hammons, D. Mathes, and R. Hull, *J. Special Topics Quan. Electron.*, 1997, vol. 3, 916.

[13] R. D. Twesten, D. M. Follstaedt, and K. D. Choquette, *SPIE Proc.*, 1997, vol. 3003, 56.

[14] R. D. Twesten, D. M. Follstaedt, K. D. Choquette, and R. P. Schneider, Jr., *Appl. Phys. Lett.*, 1996, vol. 69, 19.

[15] K. D. Choquette, K. M. Geib, H. C. Chui, B. E. Hammons, H. Q. Hou, T. J. Drummond, and R. Hull, *Applied Physics Letters*, 1996, vol. 69, 1385.

[16] K. Geib, K. D. Choquette, H. Q. Hou, and B. E. Hammons, *SPIE Proc.*, 1997, vol. 3003, 69.

[17] R. L. Naone, E. R. Hegbloom, B. J. Thibeault, and L. A. Coldren, *Electron. Lett.*, 1997, vol. 33, 300.

[18] K. D. Choquette, K. L. Lear, R. P. Schneider, K. M. Geib, J. J. Figiel, and R. Hull, *Photon. Tech. Letters*, 1995, vol. 7, 1237.

[19] K. D. Choquette, K. L. Lear, R. P. Schneider, and K. M. Geib, *Applied Physics Letters*, 1995, vol. 66, 3413.

[20] K. L. Lear, K. D. Choquette, R. P. Schneider, Jr., S. P. Kilcoyne, and K. M. Geib, *Electronics Letters*, 1995, vol. 31, 208.

[21] K. L. Lear, A. Mar, K. D. Choquette, S. P. Kilcoyne, R. P. Schneider, Jr., and K. M. Geib, *Electron. Lett.*, 1996, vol. 32, 457.